JPET Fast Forward. Published on June 8, 2012 as DOI:10.1124/jpet.112.196451

JPET #196451

PRODUCTION AND ACTIONS OF THE ANANDAMIDE METABOLITE, PROSTAMIDE E2, IN THE RENAL MEDULLA

Joseph K. Ritter, Cao Li, Min Xia, Justin L. Poklis, Aron H. Lichtman, Rehab A. Abdullah, William L. Dewey, and Pin-Lan Li

Department of Pharmacology and Toxicology,

Medical College of Virginia Campus

Virginia Commonwealth University,

Richmond, VA 23298-0613.

Running title: Anandamide and prostamide E2 in the renal medulla

*__Corresponding author__: Joseph K. Ritter, Ph.D., Virginia Commonwealth University, Department of Pharmacology and Toxicology, 1217 E. Marshall St., Medical Sciences Bldg., Room 531, P.O. Box 980613, Richmond, VA 23298-0613. Telephone: (804) 828-1022; Fax number: (804) 828-0676. Email: jkritter@vcu.edu

Number of text pages: 31

Number of tables: 0

Number of figures: 7

Number of references: 36

Number of words in abstract: 238

Number of words in introduction: 748

Number of words in discussion: 1500

Non-standard abbreviations: AEA, anandamide; Ang II, angiotensin II; COX, cyclooxygenase; FAAH, fatty acyl amide hydrolase; LC-MS/MS, liquid chromatography tandem mass spectrometry; MAP, mean arterial pressure; RBF, renal blood flow.

Recommended section assignment: Gastrointestinal, hepatic, pulmonary, and renal

ABSTRACT

Medullipin has been proposed to be an antihypertensive lipid hormone released from the renal medulla in response to increased arterial pressure and renal medullary blood flow. Since anandamide (AEA) possesses characteristics of this purported hormone, the present study tested the hypothesis that AEA or one of its metabolites represents medullipin. AEA was demonstrated to be enriched in the kidney medulla compared to cortex. Western blotting and enzymatic analyses of renal cortical and medullary microsomes revealed opposite patterns of enrichment of two AEA-metabolizing enzymes, with fatty acid amide hydrolase higher in the renal cortex and cyclooxygenase-2 (COX-2) higher in the renal medulla. In COX-2 reactions with renal medullary microsomes, prostamide E2, the ethanolamide of prostaglandin E2, was the major product detected. Intramedullarily-infused AEA dose-dependently increased urine volume and sodium and potassium excretion (15-60 nmol/kg/min) but had little effect on mean arterial pressure (MAP). The renal excretory effects of AEA were blocked by intravenous infusion of celecoxib (0.1 μg/kg/min), a selective COX-2 inhibitor, suggesting the involvement of a prostamide intermediate. Plasma kinetic analysis revealed longer elimination half-lives for AEA and prostamide E2 compared to prostaglandin E2. Intravenous prostamide E2 reduced MAP and increased renal blood flow (RBF), actions opposite to those of angiotensin II. Co-infusion of prostamide E2 inhibited angiotensin II effects on MAP and RBF. These results suggest that AEA and/or its prostamide metabolites in the renal medulla may represent medullipin, and function as a regulator of body fluid and MAP.

INTRODUCTION

The concept that the kidney is the most important organ for long-term blood pressure control and that renal dysfunction is a major cause of hypertension has gained increasing acceptance. Whereas the pro-hypertensive hormonal system of the kidney, i.e., the renin-angiotensin system, is well established, the kidney has also been proposed to contain an antihypertensive endocrine system (Muirhead, 1993). According to this hypothesis, the renal medulla responds to increased medullary blood flow by secreting a vasodepressor lipid termed medullipin. The antihypertensive effects of medullipin were proposed to be due to three specific biologic properties: vasodilator, inhibitor of sympathetic activation, and promoter of renal salt and water excretion. Others have speculated on a possible relationship between medullipin and the mechanism of pressure natriuresis, whereby sodium and water excretion by the kidneys are increased in proportion to elevated renal perfusion pressure (Mattson, 2003). With respect to pressure natriuresis, it is known that glomerular filtration, total RBF and cortical blood flow are finely regulated and do not change significantly in response to increased renal perfusion pressure, whereas medullary blood flow is poorly autoregulated and increases in proportion to elevated renal perfusion pressure. Pressure natriuresis is a local renal adaptive mechanism to increased arterial blood pressure. However, the identity of medullipin has remained elusive, but its elucidation undoubtedly has great potential to lead to new therapies for hypertension.

The present study tested the hypothesis that anandamide (AEA) or/and its metabolites represent medullipin. AEA is the N-acyl ethanolamide of arachidonic acid. Best known as a major endocannabinoid in the brain (Devane et al.., 1992), AEA has been noted for its high concentration in kidney (Koga et al., 1997; Long et al., 2011), though its distribution in this organ has not been established. Whereas roles for AEA have been identified for various physiological responses, such as

antinociception (Cravatt et al., 2001), drug dependence (Schlosburg et al., 2009a; Ramesh et al., 2011), and inflammation (Schlosburg et al., 2009b), its functions in the kidney are not well defined.

AEA has several characteristics consistent with the biological identity of medullipin. First, it is a neutral lipid and a derivative of arachidonic acid (Muirhead, 1993). After intravenous infusion into anesthetized rats, AEA elicited a prolonged vasodepressor response accompanied by bradycardia, consistent with inhibition of the baroreceptor reflex and sympathetic outflow (Varga et al., 1995). Indeed, the vasorelaxant properties of AEA have been demonstrated on various arteriolar beds (Mair et al., 2010) including afferent and efferent arterioles of the kidney (Deutsch et al., 1997) (Koura et al., 2004). Deutsch et al. (1997) showed that AEA inhibits the KCl-stimulated release of norepinephrine from sympathetic nerves on renal arterioles, consistent with its ability to inhibit sympathetic effector function. Finally, methanandamide, a methylated analogue of AEA, increased urine volume and decreased mean arterial blood pressure after intra-renal medullary infusion in anesthetized rats, implying that medullary AEA can regulate body volume homeostasis and blood pressure (Li & Wang, 2006). Whereas some of the latter effects were blocked by known antagonists of AEA receptors, others such as the effect of intramedullarily infused methanandamide on diuresis and blood pressure were not, suggesting a cannabinoid receptor-independent mechanism.

The kidney is also unique in its high activities of the AEA-metabolizing enzymes, fatty acid amide hydrolase (FAAH) and cyclooxygenase-2 (COX-2). FAAH is a membrane-bound amidase that catalyses the hydrolysis of AEA to arachidonic acid and ethanolamine (Cravatt et al., 2001). FAAH is usually considered as an AEA-inactivating enzyme, because its products are inactive at cannabinoid receptors. However, arachidonic acid is itself an enzyme substrate and signaling molecule. COX-2, the “inducible” form of cyclooxygenase, is expressed constitutively in the kidney (Harris et al., 1994), particularly in the renal medulla (Yang, 2003). COX-2 was demonstrated to metabolize AEA to N-ethanolamide analogues of prostaglandins (Yu et al., 1997), termed “prostamides”. Whether prostamides have a functional role in

the kidney or elsewhere in the body remains unknown. However, several prostamides including prostamide E2 were detected in the kidney of mice treated with AEA (Weber et al., 2004).

The present study addressed the relationship among AEA, COX-2 and FAAH in the kidney, with a particular focus on the difference between cortex and medulla. The renal excretory effects of AEA following its infusion into the renal medulla were studied in the absence and presence of a COX-2 inhibitor. Finally, the pharmacokinetic and cardiovascular properties of prostamide E2 after intravenous infusion were characterized. Our data highlight several additional properties of AEA or its COX-2 metabolite, prostamide E2, consistent with their identity as renomedullary neutral antihypertensive lipids.

MATERIALS AND METHODS

AEA, prostamide E2, and prostamide F2 alpha were purchased from Cayman Chemical (Ann Arbor, Michigan). Arachidonic acid was from Sigma Chemical. The deuterated analogues, d_8-AEA, d_8-2-arachidonoylglycerol, and d_8-arachidonic acid, were from Cayman Chemical. All chemicals used in the study were of reagent-grade or better.

Animals: Two to four month old male mice with a C57BL6 background were used in this study. The mice were generated using a breeding colony of cannabinoid receptor and FAAH knockout mice established at Virginia Commonwealth University. The knockout strains have been maintained by backcrossing onto the C57BL6 background for approximately 12 generations. In some cases, male C57BL6/J mice purchased from The Jackson Laboratory (Bar Harbour, ME) were used. All experiments involving mice in this work were conducted according to protocols previously approved by the Virginia Commonwealth University Institutional Animal Care and Use Committee.

Liquid chromatography tandem mass spectrometry (LC–MS/MS) for quantitation of endocannabinoids and fatty acyl amides: The endocannabinoids, AEA and 2-arachidonoyl glycerol, and the ethanolamides of the fatty acids, oleic acid, and palmitic acid, were measured in renal cortex and medulla by LC-MS/MS as described (Ramesh et al., 2011). Briefly, mice were euthanized, the kidneys

removed, and the renal cortex and medulla rapidly dissected on ice, snap frozen in liquid nitrogen, and stored at -80C until the time of processing. On the day of processing, the preweighed tissues were homogenized in 1.4 mL chloroform/methanol (2:1 v/v containing 0.2 M phenylmethylsulfonyl fluoride with 2 pmol d_8-AEA, 1 nmol d_8-2-arachidonoyl glycerol, 3.3 nmol d_4-palmitoyl ethanolamide, 3 nmol d_4-oleoyl ethanolamide, and 1 nmol d_8-arachidonic acid as internal standards. After adding ice cold normal saline (0.3 mL), the samples were vortexed for 1 min, and the tubes were then centrifuged at 3200 x g at 4°C for 10 min. The organic phase was collected, and the aqueous phase plus debris were extracted two more times with 0.8 mL of chloroform. The organic phases from the three extractions were pooled and dried under nitrogen gas, and the residue was reconstituted with 0.1 mL of chloroform and mixed with 1 mL ice-cold acetone. After centrifuging at 1800 x g for 5 min at 4°C, the upper layer was collected and evaporated under nitrogen. Dried samples were reconstituted with 0.1 mL of methanol for analysis by LC-MS/MS in electrospray mode. The following ion transitions were monitored in positive mode, (348>62) and (348>91) for AEA ; (356>62) for AEA-d8; (379>287) and(279>269) for 2-AG ; (387>96) for 2AG-d8; (300>62) and (300>283) for PEA; (304>62) for PEA-d4; (326>62) and (326>309) for OEA; and (330>66) for OEA-d4; and in negative mode : (303>259) and (303>59) for AA and (311>267) for AA-d8. A calibration curve was constructed for each assay based on peak area ratios for the calibrators and internal standards. The extracted standard curves ranged from 0.03 to 40 pmol for AEA and from 0.05 to 64 nmol for 2-arachidonoyl glycerol.

Immunohistochemical analysis for COX-2 and FAAH in the mouse kidney: The kidneys were removed, cut longitudinally, and fixed in 10% neutral buffered formalin. The fixed tissue was embedded in paraffin, and 4-μm sections were cut. Immunostaining was performed as described previously (Li et al., 2007) using a rabbit anti-COX-2 polyclonal antibody (Cat. No. 4842, 1:50, Cell Signaling Technology, Beverly, Massachusetts) or a rabbit monoclonal anti-FAAH antibody (Cat. No. 3829, 1:2000 dilution; Cell Signaling Technology), respectively. For a negative control, normal goat or rabbit serum was used instead. The negative controls did not show positive immunoreactivity.

Prostamide-forming activity in kidney microsomes with AEA as substrate: Kidney cortical and medullary tissues from 4-6 mice were pooled and homogenized in ice-cold 0.25 M sucrose containing 25 mM Na-HEPES, pH 7.4, 1mM EDTA, and Complete® protease inhibitor cocktail (Roche, Mannheim, Germany). After centrifuging at 10,000 g for 10 min at 4°C, the supernatant was transferred and centrifuged at 100,000 x g for 1 hr. The microsomes were resuspended in the same buffer, aliquotted into several tubes, snap frozen in liquid nitrogen, and stored at −80°C. The microsomal protein concentration was determined by the Bradford method using a commercially available kit (Bio-Rad, Hercules, CA).

Reactions (100 μL) contained 1 mg/mL microsomal protein, 0.1 M Tris-HCl, pH 8.0, 1 mM epinephrine, 1 mM glutathione and 0.1 mM AEA. The reactions were incubated at 37°C for 30 min and stopped by the addition of 15 μL 2N HCl followed by 300 μL 2:1 (v/v) chloroform/ methanol. The samples were vortexed for 90 sec and centrifuged for 3 min. The bottom layer was transferred to a glass conical tube, and d_8-AEA (5 ng) was added as external standard. The samples were dried under nitrogen gas and reconstituted in methanol for analysis by LC-MS/MS as described (Weber et al., 2004) with some modification. The flow rate was 0.2 mL/min. The column was a Luna C8 3 μm (100 x 2.0 mm) column maintained at 40°C temperature. The entire liquid chromatography eluent was directed into the electrospray ionization source. The mass spectrometer was switched between positive ion mode (for AEA, prostamides and d8-AEA) and negative ion mode (for arachidonic acid). The ion transitions monitored were: (396 > 378) and (396 > 62) for prostamide E2; (356 > 62) for AEA-d8; (398 > 380) and (398 > 62) for prostamide F2α; and (303>259) for arachidonic acid. Calibration curves were constructed for prostamide E2 and arachidonic acid.

Western blot analysis: Western blot analysis was performed as previously described (Zou et al., 2001). Briefly, kidney cortical or medullary microsomal samples (20 μg) were electrophoresed through an SDS-PAGE gel together with a protein size standard followed by electroblotting onto a nitrocellulose membrane. The membrane was probed for FAAH or COX-2 protein using the anti-FAAH or anti-COX-2 antibodies described above at 1:2000 and 1:50 dilutions, respectively. After washing, the membranes

were incubated for 1 h with 1:3000 horseradish peroxidase-labeled secondary antibody. Images were developed using enhanced chemiluminescence detection solution (ECL, Pierce) followed by exposure to Kodak X-Omat Blue film. The intensities of the protein bands on the image were quantified using NIH ImageJ analysis software. To normalize for small differences in protein loading, the blots were stripped and reanalyzed with an anti-β-actin primary antibody (1:2000 dilution, Sigma Chemical Co.).

Surgical preparation of mice: Mice were anesthetized and prepared surgically for each of the following protocols as described (Li et al., 2005). Briefly, after anesthesia with ketamine (Ketaject; 30 mg/kg, i.p.) and thiobutabarbital (Inactin; 50 mg/kg, i.p.), the mice were placed on a thermostatically controlled warming table to maintain body temperature at 37°C. After tracheotomy, catheters were placed in the jugular vein and carotid artery for intravenous infusions and measurements of MAP, respectively. For experiments where RBF was measured, a flow probe (2 mm, Transonic Systems) was placed around the left renal artery and RBF was measured as described previously.

Protocol 1: Intramedullary interstitial infusion of AEA and measurement of MAP, urinary formation, and RBF: The technique for construction and placement of a catheter for renal medullary infusion (Lu et al., 1992) is well established in our laboratory (Li et al., 2005; Zhu et al., 2011). Briefly, the left kidney was immobilized by placement of its dorsal side up in a kidney cup. A catheter (tapered tip, 1 mm) was gently implanted into the renal outer medulla vertically from the dorsal surface and anchored into place on the kidney surface with Vetbond Tissue Adhesive (3M Co., Minneapolis, MN). The medullary catheter was infused with solution containing 90% phosphate buffered saline containing (in mM) 205 NaCl, 40.5 Na_2HPO4, and 9.5 NaH_2PO4 (pH 7.4, 550 mosM), 5% ethanol and 5% Emulphor at a rate of 2 μl/min to maintain the patency of interstitial infusion line. For the collection of urine from the left kidney, the right ureter was ligated and then cut to keep open on the side proximal to the kidney, and the bladder was catheterized to collect urine. The urine volume (U·V) was determined gravimetrically and urinary sodium (Na^+) and potassium (K^+) concentrations were measured by flame photometry. Urine volume (U·V) and urinary Na^+ excretion (UNa·V) were factored per gram kidney

weight. Mice received a continuous intravenous infusion of 0.9% NaCl solution containing 2% albumin at a rate of 1 mL·h^{-1}·100 g body wt^{-1} to replace fluid loss and maintain a constant hematocrit (≈42%). After a 1.5-h equilibration period and two 10-min control sample collection periods during infusion of the vehicle alone, AEA was infused for 30 min periods (10-min dead space removing period and 20-min sample collection) at three doses (15, 30 and 60 nmol/kg/min). The AEA was first dissolved in ethanol and then in Emulphor and 550 mOsm saline-phosphate solution for final concentrations of 5%, 5%, and 90%, respectively. The vehicle without AEA was infused during equilibration period. An additional group of mice was infused intravenously with the COX-2 selective inhibitor, celecoxib, Sigma Chemical) at 0.1 μg/min/kg in the intravenous vehicle starting with the control infusion periods. This surgical preparation and protocol procedure have been widely used in the studies of renal physiology and infusion of vehicle alone does not produce any significant change in renal function over the period of testing. At the end of the experiment, the mice were euthanized by an anesthetic overdose (Inactin). The left kidney was excised and weighed, and the position of the medullary catheter was confirmed.

Protocol 2: Effects of intravenous prostamide E2 on MAP and RBF. After surgical preparation of the mice and a 1.5-h equilibration and 20-min control sample collection periods with intravenous infusion of vehicle alone, prostamide E2 dissolved in vehicle was infused intravenously at 30, 60 or 120 nmol/kg/min, and its effects on MAP and RBF were measured.

Protocol 3: Effects of prostamide E2 on angiotensin (Ang) II-induced elevation of MAP and decrease in RBF. Mice were surgically prepared as described above. The effect of Ang II delivered intravenously either as a bolus (50 ng/kg) or continuously (10, 20 or 40 ng/kg/min) on MAP and RBF was determined. The effect of prostamide E2 given intravenously (120 nmol/kg/min) on the Ang II responses was determined.

Pharmacokinetic analysis of AEA and prostamide E2 plasma elimination in mice: The plasma elimination of AEA and prostamide E2 was evaluated in conscious mice after intravenous administration

of bolus doses of 3.6 μmol/kg of either compound by injection into the tail vein. The vehicle was 5% ethanol-5% Emulphor-90% saline (1 mL/kg). Timed serial blood samples (50 μL) were removed from the tail vein at 5, 15, 30, 60 and 120 min after injection into EDTA tubes. Plasma was collected by centrifugation, and 25 μL was extracted and analyzed for AEA or prostamide E2 by LC-MS/MS as described above.

Statistical analyses: The data are presented as the mean ± standard error of the mean. For comparisons among multiple groups of data, the significant difference was determined by using one-way or two-way ANOVA followed by the Tukey-Kramer post hoc test. For comparisons between two groups of data, a Students' t-test was used to detect significant differences. Only comparisons having a p value ≤ 0.05 were considered statistically significant.

RESULTS

Levels of AEA and 2-arachidonoyl glycerol (2-AG) in mouse renal cortex and medulla. To assess the distribution of AEA in the kidney, the cortex and medulla from kidneys of C57BL6 mice were dissected and analyzed for endocannabinoids and other fatty acyl ethanolamides (Fig. 1). The AEA level was 2.4-fold higher in the renal medulla compared to the cortex (26.0 vs. 10.7 pmol/g, $p<0.05$). Two other fatty acyl ethanolamides, oleoyl ethanolamide and palmitoyl ethanolamide, were also higher in the renal medulla than in cortex (3.3 and 4.6-fold, respectively, $p<0.05$). In contrast, 2-arachidonyl glycerol levels did not differ between the renal cortex and medulla (11.4 and 10.4 nmol/g, respectively).

Distribution of COX-2 and FAAH in the renal cortex and medulla. The distributions of the COX-2 and FAAH proteins in microsomes prepared from the kidney were studied by Western blot analysis and immunohistochemical localization (Fig. 2). In the Western analysis (Fig. 2A), immunoreactive bands consistent with FAAH (61 kDa) and COX-2 (74 kDa) were detected in the kidney microsomes. The two proteins showed opposite abundance profiles in the renal cortex compared to medulla with the FAAH immunoreactive band more intense in the cortex microsomes, and the COX-2 band more intense in

medulla microsomes. Quantitation using β-actin as a normalizing control indicated 3.6-fold higher FAAH protein in the cortex compared to medulla, and 6.1-fold higher COX-2 in the medulla compared to cortex (Fig. 2B, $p<0.05$). The results of immunohistochemical analyses of FAAH and COX-2 were in good agreement with the Western blot findings (Fig. 2C). FAAH immunostaining was most intense in the cortex region, with both proximal and distal tubule cells showing positive staining, in contrast to the weak or absent staining of cells in glomerular structures. In the medulla, FAAH staining was more selective, appearing to be limited to collecting ducts. The staining pattern with COX-2 in the cortex compared to the medulla was distinct from that of FAAH (Fig. 2C, lower panels). In the renal cortex, positive COX-2 staining was limited to scattered cells or groups of cells in thick ascending limb tubules, particularly in regions where these cells came into contact with or were in proximity to glomeruli. This staining pattern is consistent with the reported expression of COX-2 in cells of the macula densa. In the medulla, COX-2 positive staining was detected in tubular segments with weak or otherwise minimal staining of collecting ducts.

Hydrolysis and prostamide E2 formation from AEA by cortical and medullary microsomes. Fig. 3 presents a comparison of the rates of AEA hydrolysis to arachidonic acid and oxidation to prostamide E2 by cortical and medullary microsomes with representative chromatograms. The kidney cortical microsomes showed a significantly higher rate of AEA-dependent arachidonic acid formation compared to medullary microsomes (928±98 vs. 787±79 pmol/mg/hr, respectively) (Fig. 3A), consistent with the cortex having higher FAAH activity. In contrast, the renal medulla microsomes were more active than cortical ones in forming prostamide E2 (33.4±7.5 vs. 20.4±3.8 pmol/mg/hr, respectively, $p<0.05$) (Fig. 3B). Prostamide E2 was not detected in reactions containing microsomes only or reaction components only (data not shown).

Effect of medullary infusion of AEA on blood pressure, urine volume and sodium excretion and its inhibition by a selective COX-2 inhibitor. An acute renal function study was performed using anesthetized mice with surgically implanted catheters for measuring renal perfusion pressure and urine

formation. These results are presented in Fig. 4. Following a 1.5-hr equilibration period and two 15-min control periods (labeled C1 and C2 in Fig. 4), addition of AEA to the medullary infusion solution was tested. Medullary infusion of AEA had little apparent effect on blood pressure, but increased urine flow and sodium and potassium excretion adjusted for kidney weight. The effects of AEA were dose-dependent between 15 to 60 nmol/kg/min. Removal of the AEA from the medullary infusion solution resulted in the urine flow and sodium excretion values returning toward the control level. Pretreatment of the mice with an intravenous infusion of celecoxib, a COX-2 selective inhibitor, at a rate of 0.1 μg/kg/min for 30 min completely blocked the effects of AEA on both urine flow and excretion of sodium and potassium. This observation suggests that COX-2 metabolites of AEA mediate the diuretic and natriuretic effects of AEA during its intramedullary infusion in the mouse kidney.

Kinetics of AEA and prostamide E2 after intravenous bolus injection. Plasma samples from control C57BL6 mice before and after intravenous bolus doses of AEA or prostamide E were analyzed for AEA and prostamide E2 levels (Fig. 5). Basal levels of AEA (3-8 nmol/L) but not prostamide E2 (data not shown) were detectable in plasma collected immediately prior to the bolus i.v. injection (3-8 nmol/L, 1-3 ng/mL). After an i.v. AEA bolus (3.6 mg/kg, Fig. 5A), AEA exhibited a peak plasma level by 5 min after administration (489 ng/mL), which declined subsequently with a half-life of 20-30 min. No prostamide E2 was detected in the plasma of the AEA-injected mice. Intravenous injection of a prostamide E2 bolus resulted in a maximum plasma concentration of prostamide E2 by 5 min after injection (141 ng/mL, Fig. 5B). There was no apparent change in plasma AEA concentration after prostamide E2 dosing, consistent with the COX-2 metabolite being resistant to FAAH-mediated hydrolysis (Ritter, J.K., and Li, P.-L., unpublished data). Prostamide E2 exhibited an elimination half-life of 21 min. An unidentified prostamide E2 metabolite having identical parent ion ($[MH]^+$ 396) and product ion ($[MH]^+$ 378)) as prostamide E2 was detected in the prostamide E2 MRM chromatograms. The signal for this metabolite was only detected in mice injected with prostamide E2 and became more intense than prostamide E2 by

30 min and later time after injection, suggesting higher abundance. The elimination of this unknown isomeric metabolite paralleled that of prostamide E2 (half-life of 26 min).

Effect of intravenous prostamide E2 infusion on blood pressure and RBF. The influence of intravenously infused prostamide E2 on MAP and RBF was investigated in anesthetized mice. Representative blood pressure and RBF tracings from a single animal showing the effects of prostamide E2 on these parameters are shown in Fig. 6A. Prostamide E2 had modest, but statistically significant, effects on MAP and RBF under control conditions. At the highest dose tested (120 nmol/kg/min) prostamide E2 decreased MAP by 7% from 99.4 mmHg to 92.6 mmHg and increased RBF by 23% (4.7 to 5.8 mL/min/g kidney weight) (Fig. 6B).

Inhibition of Ang II-mediated increases in MAP and reductions of RBF by prostamide E2. The influence of prostamide E2 was also evaluated on Ang II-induced elevation in MAP and reduction of RBF. Administration of the Ang II bolus transiently elevated MAP and decreased RBF, but both these effects were inhibited by prostamide E2 (see Fig. 7A for representative tracings). The summarized data in Fig. 7B show that, whereas the Ang II bolus alone elevated MAP by an average 22 mm Hg, this response was reduced 46% to 12 mm Hg by prostamide E2 (Fig. 7B, left panel). Similarly, Ang II reduced RBF by 48% (4.6 to 2.4 mL/min/g kidney weight) in the presence of vehicle, and by 23% (5.3 to 4.2 mL/min/g kidney weight) in the presence of infused prostamide E2 (Fig. 7B, right panel). Similar antagonistic effects of prostamide E2 were observed when Ang II was administered by continuous i.v. infusion. In tracings from a representative animal (Fig. 7C), infusion of Ang II at increasing concentration (5, 10, and 20 ng/kg/min) elevated MAP and decreased RBF in a concentration-dependent manner (Fig. 7C, left panel), and these effects were inhibited by the presence of prostamide E2 (Fig. 7C, right panel). Summarized data showing significant inhibition of Ang II effects at the intermediate and high Ang II concentrations are shown in Fig. 7D.

DISCUSSION

The purpose of this study was to evaluate AEA and its prostamide metabolites for their possible relationship to the renomedullary neutral antihypertensive lipid, “medullipin” (Muirhead, 1993). The observation that AEA is enriched in the mouse renal medulla relative to cortex (Fig.1A) has not been previously described. The AEA enrichment in the renal medulla is not clearly understood but may be due to relatively low levels of FAAH in medullary cells. The presence of AEA in neurons is well known, but it is also present in cells that are non-neuronal in origin (Liu et al., 2006). In the kidney, AEA has been identified in cultured renal microvascular endothelial cells and in glomerular mesangial cells (Deutsch et al., 1997). Based on the hypothesis that AEA or an AEA metabolite represents medullipin, it may be speculated that AEA is present in the lipid-rich granules of renomedullary interstitial cells, the proposed source of medullipin, but further studies are needed to confirm this possibility.

It was also of interest to evaluate the distribution in the kidney of two known AEA-metabolizing enzymes, namely, FAAH and COX-2, in relation to that of AEA. Multiple lines of evidence support opposing patterns of FAAH and COX-2 expression in the renal cortex and medulla. FAAH protein (Fig. 2) and a measure of its activity, hydrolysis of AEA to arachidonic acid (Fig. 3), were higher in the cortex than medulla, whereas the pattern for COX-2 was opposite. Although the kidney has been reported to have high FAAH (Long et al., 2011), its localization in the kidney has never been studied to our knowledge. FAAH immunostaining was strong in various cortical tubular segments including proximal convoluted tubule, thick ascending limbs of the Loop of Henle, and cortical distal and connecting tubules. Some positive staining of FAAH was evident in glomeruli, but the intensity was lower than that in tubules. These immunohistochemical-based observations agree with the higher FAAH levels observed by Western blotting and enzymatic analysis. Increased FAAH activity in the renal cortex could at least in part explain the relatively low levels of AEA there and suggests the physiologic importance for maintaining low AEA concentrations in the renal cortex. Alternatively, AEA in conjunction with high FAAH in the renal cortex could serve as a source of arachidonic acid for prostaglandin synthesis in the tubuloglomerular feedback mechanism (Araujo & Welch, 2009). In the renal medulla, the inner

medullary collecting ducts exhibited intense positive FAAH immunostaining. Further research is necessary to understand the role of FAAH and the regulation of AEA synthesis and release in the cortical and medullary regions of kidney.

In contrast, the COX-2 protein and an associated enzymatic activity--conversion of AEA to prostamide E2--were both higher in the renal medulla compared to cortex (Figs. 2 and 3). This differential expression of COX-2 in the renal medulla was supported by >10-fold higher COX-2 mRNA expression in renal medulla compared to the cortex (data not shown). The immunohistochemical analysis with COX-2 was less convincing, as positive COX-2 immunostained cells were only clearly visible in the renal cortex. The pattern of COX-2 immunostaining observed in our study is consistent with other reports (Harris et al., 1994). In the renal cortex, positive COX-2 staining was observed in isolated cells or clusters of cells in distal tubules adjacent to glomeruli, consistent with expression in cortical thick ascending limb cells and cells of the macula densa (Harris et al., 1994). The low COX-2 immunostaining in the mouse kidney medulla is in agreement with a previous report (Campean et al., 2003). Yet, it contrasts with the higher levels in the medulla suggested by Western and enzymatic activity analyses. Since prostamide formation from AEA is known at present only to be catalyzed by COX-2 (Yu et al., 1997), the failure to detect COX-2 in the renal medulla by immunohistochemistry may be due to COX-2 expression being too broad and diffuse to permit visualization of positive staining above background.

In the acute renal function studies, a link between AEA and COX-2 is suggested by the data (Fig. 4). When AEA was infused into the renal medulla, urine flow and sodium excretion were increased. However, this effect was completely prevented if the mice were pretreated with a selective COX-2 inhibitor. This finding indicates that a COX-2 metabolite of AEA indirectly mediates the renal excretory effects of AEA. Using a similar experimental approach in rats, Li and Wang (2006) showed that the intramedullary infusion of the methyl analogue of AEA, methanandamide, stimulated urine volume and reduced MAP (Li & Wang, 2006). Methandamide has similar cannabinoid receptor-stimulating specificity to AEA but is resistant to FAAH-mediated hydrolysis (Abadji et al., 1994). The effect of

intramedullarily-infused methanandamide was not blocked by pretreatment with either a cannabinoid receptor-1 or vanilloid receptor antagonist, indicating a unique mechanism. It is plausible that this cannabinoid-independent mechanism for methanandamide also involves its conversion to COX-2 metabolites, as methanandamide is also an efficient COX-2 substrate (Kozak et al., 2003). Further studies are needed to determine which COX-2 metabolites of AEA underlie the mechanism of its diuresis and natriuresis after its infusion into the renal medulla.

According to the hypothesis of Muirhead (Muirhead et al., 1991), medullipin is secreted from the renal medulla into the blood to elicit antihypertensive effects through its properties as a vasodepressor and inhibitor of sympathetic activity. Prostaglandin E2, the major renal vasodilatory factor, was excluded as a candidate for this mechanism, based in part on its ultra-short duration of activity in plasma, on the order of seconds (Ferreira & Vane, 1967; Hamberg & Samuelsson, 1973). In this study, the plasma kinetics of AEA and its major renal prostamide metabolite, prostamide E2, were evaluated in mice (3.6 μmol/kg). In contrast to prostaglandin E2 which disappears completely from the plasma within 4-6 min (Hamberg & Samuelsson, 1971), both AEA and prostamide E2 remained detectable in plasma for at least 1 h following a bolus injection (Fig. 5). Estimates of the plasma half-lives for AEA and prostamide E2 were 21 and 27 min, respectively. The half-life of prostamide E2 measured in normal mice is more than 4-fold longer than the ~ 6 min half-life in rats given a comparable dose (2 mg/kg) (Kozak et al., 2002). The relative resistance of prostamide E2 to elimination is consistent with the idea that prostamides are released into the blood to exert effects at sites distant from their tissue of origin (Kozak et al., 2001; Weber et al., 2004). In this study, a metabolite of prostamide E2 was observed which has an identical [M+H]+ mass to charge ratio and slightly higher lipophilicity. Given that the two main pathways of prostaglandin metabolism are dehydrogenation of the 15-hydroxyl group and reduction of the 13,14-double bond (Dunn & Hood, 1977), the observed metabolite could be explained by similar reactions acting in sequence. The extent to which this pathway contributes to the plasma clearance of prostamide E2 as well as its potential contribution to the biological activity of prostamides remains open to investigation.

Muirhead and colleagues (Muirhead et al., 1991) proposed that medullipin and Ang II were physiological counterparts having opposite effects on vasomotor tone, sympathetic activity, and salt and water retention by the kidney. AEA given by intravenous bolus (4 mg/kg) to anesthetized rats elicits a triphasic response, including a prolonged depressor third phase that was attributed to cannabinoid receptor-1-mediated inhibition of sympathetic outflow (Varga et al., 1995). In addition, multiple studies have reported vasorelaxant effects of AEA in various arteriolar resistance beds (Mair et al., 2010). In this study, we showed that prostamide E2 given in a continuous infusion modestly decreased MAP and increased RBF (Fig.6), which was opposite to those of Ang II. Further study is needed to determine if the mechanism of this novel observation is due to direct vasorelaxation or inhibition of sympathetic tone and to determine the receptors that mediate the effect of prostamide E2, possibly prostaglandin E2 receptors (Ross et al., 2002). Additional data conclusively demonstrate that prostamide E2 can directly reverse Ang II-induced pressor response and reduction of RBF (Fig. 7). Although further studies are needed to explore the molecular mechanisms, the counteracting actions of prostomide E2 on Ang II-induced hemodynamic response are consistent with the nature of medullipin as proposed by Muirhead and colleagues.

In summary, the results of the present study demonstrate that AEA or one of its COX-2-metabolites, namely, prostamide E2, shares several properties in common with those proposed for medullipin, the antihypertensive lipid with vasodilator, sympatholytic, and diuretic/natriuretic actions. In addition to its neutral lipid character, its close relationship to arachidonic acid, and an apparent role for metabolism in mediating its antihypertensive effects, we showed that AEA infused in the renal medulla is diuretic and natriuretic and this effect is mediated by COX-2. Thus, we propose that AEA or prostamide E2 may represent medullipin. A key to this hypothesis is that AEA or its COX-2 metabolite(s) are synthesized in the renal medulla and released in response to increases in renal medullary blood flow. Studies in our laboratory are ongoing to address this key issue.

Authorship Contributions:

Participated in research design: C. Li, Xia, Ritter, Lichtman, Dewey, P-L. Li

Conducted experiments: C. Li, Xia, Ritter, Abdullah, Poklis

Performed data analysis and interpretation: C. Li, Xia, Ritter, Lichtman, Dewey, Abdullah, Poklis, P-L. Li

Contributed to the writing of the manuscript: C. Li, Xia, Ritter, Lichtman, Abdullah, Poklis, Dewey, P-L. Li

REFERENCES

Abadji V, Lin S, Taha G, Griffin G, Stevenson LA, Pertwee RG, Makriyannis A (1994) (R)-methanandamide: a chiral novel anandamide possessing higher potency and metabolic stability. *J Med Chem* **37:** 1889-1893

Araujo M, Welch WJ (2009) Cyclooxygenase 2 inhibition suppresses tubuloglomerular feedback: roles of thromboxane receptors and nitric oxide. *Am J Physiol Renal Physiol* **296:** F790-794

Campean V, Theilig F, Paliege A, Breyer M, Bachmann S (2003) Key enzymes for renal prostaglandin synthesis: site-specific expression in rodent kidney (rat, mouse). *Am J Physiol Renal Physiol* **285:** F19-32

Cravatt BF, Demarest K, Patricelli MP, Bracey MH, Giang DK, Martin BR, Lichtman AH (2001) Supersensitivity to anandamide and enhanced endogenous cannabinoid signaling in mice lacking fatty acid amide hydrolase. *Proc Natl Acad Sci U S A* **98:** 9371-9376

Deutsch DG, Goligorsky MS, Schmid PC, Krebsbach RJ, Schmid HH, Das SK, Dey SK, Arreaza G, Thorup C, Stefano G, Moore LC (1997) Production and physiological actions of anandamide in the vasculature of the rat kidney. *J Clin Invest* **100:** 1538-1546

Devane WA, Hanus L, Breuer A, Pertwee RG, Stevenson LA, Griffin G, Gibson D, Mandelbaum A, Etinger A, Mechoulam R (1992) Isolation and structure of a brain constituent that binds to the cannabinoid receptor. *Science* **258:** 1946-1949

Dunn MJ, Hood VL (1977) Prostaglandins and the kidney. *Am J Physiol* **233:** 169-184

Ferreira SH, Vane JR (1967) Prostaglandins: their disappearance from and release into the circulation. *Nature* **216:** 868-873

Hamberg M, Samuelsson B (1971) On the metabolism of prostaglandins E 1 and E 2 in man. *J Biol Chem* **246:** 6713-6721

Hamberg M, Samuelsson B (1973) Detection and isolation of an endoperoxide intermediate in prostaglandin biosynthesis. *Proc Natl Acad Sci U S A* **70:** 899-903

Harris RC, McKanna JA, Akai Y, Jacobson HR, Dubois RN, Breyer MD (1994) Cyclooxygenase-2 is associated with the macula densa of rat kidney and increases with salt restriction. *J Clin Invest* **94:** 2504-2510

Koga D, Santa T, Fukushima T, Homma H, Imai K (1997) Liquid chromatographic-atmospheric pressure chemical ionization mass spectrometric determination of anandamide and its analogs in rat brain and peripheral tissues. *J Chromatogr B Biomed Sci Appl* **690:** 7-13

Koura Y, Ichihara A, Tada Y, Kaneshiro Y, Okada H, Temm CJ, Hayashi M, Saruta T (2004) Anandamide decreases glomerular filtration rate through predominant vasodilation of efferent arterioles in rat kidneys. *J Am Soc Nephrol* **15:** 1488-1494

Kozak KR, Crews BC, Morrow JD, Wang LH, Ma YH, Weinander R, Jakobsson PJ, Marnett LJ (2002) Metabolism of the endocannabinoids, 2-arachidonylglycerol and anandamide, into prostaglandin, thromboxane, and prostacyclin glycerol esters and ethanolamides. *J Biol Chem* **277:** 44877-44885

Kozak KR, Crews BC, Ray JL, Tai HH, Morrow JD, Marnett LJ (2001) Metabolism of prostaglandin glycerol esters and prostaglandin ethanolamides in vitro and in vivo. *J Biol Chem* **276:** 36993-36998

Kozak KR, Prusakiewicz JJ, Rowlinson SW, Prudhomme DR, Marnett LJ (2003) Amino acid determinants in cyclooxygenase-2 oxygenation of the endocannabinoid anandamide. *Biochemistry* **42:** 9041-9049

Li J, Wang DH (2006) Differential mechanisms mediating depressor and diuretic effects of anandamide. *J Hypertens* **24:** 2271-2276

Li N, Yi F, Sundy CM, Chen L, Hilliker ML, Donley DK, Muldoon DB, Li PL (2007) Expression and actions of HIF prolyl-4-hydroxylase in the rat kidneys. *Am J Physiol Renal Physiol* **292:** F207-216

Li N, Zhang G, Yi FX, Zou AP, Li PL (2005) Activation of NAD(P)H oxidase by outward movements of H+ ions in renal medullary thick ascending limb of Henle. *Am J Physiol Renal Physiol* **289:** F1048-1056

Liu J, Wang L, Harvey-White J, Osei-Hyiaman D, Razdan R, Gong Q, Chan AC, Zhou Z, Huang BX, Kim HY, Kunos G (2006) A biosynthetic pathway for anandamide. *Proc Natl Acad Sci U S A* **103:** 13345-13350

Long JZ, LaCava M, Jin X, Cravatt BF (2011) An anatomical and temporal portrait of physiological substrates for fatty acid amide hydrolase. *J Lipid Res* **52:** 337-344

Lu S, Roman RJ, Mattson DL, Cowley AW, Jr. (1992) Renal medullary interstitial infusion of diltiazem alters sodium and water excretion in rats. *Am J Physiol* **263:** R1064-1070

Mair KM, Robinson E, Kane KA, Pyne S, Brett RR, Pyne NJ, Kennedy S (2010) Interaction between anandamide and sphingosine-1-phosphate in mediating vasorelaxation in rat coronary artery. *Br J Pharmacol* **161:** 176-192

Mattson DL (2003) Importance of the renal medullary circulation in the control of sodium excretion and blood pressure. *Am J Physiol Regul Integr Comp Physiol* **284:** R13-27

Muirhead EE (1993) Renal vasodepressor mechanisms: the medullipin system. *J Hypertens Suppl* **11:** S53-58

Muirhead EE, Brooks B, Byers LW, Brown P, Pitcock JA (1991) Medullipin system. Generation of medullipin II by isolated kidney-liver perfusion. *Hypertension* **18:** III158-163

Ramesh D, Ross GR, Schlosburg JE, Owens RA, Abdullah RA, Kinsey SG, Long JZ, Nomura DK, Sim-Selley LJ, Cravatt BF, Akbarali HI, Lichtman AH (2011) Blockade of endocannabinoid hydrolytic enzymes attenuates precipitated opioid withdrawal symptoms in mice. *J Pharmacol Exp Ther* **339:** 173-185

Ross RA, Craib SJ, Stevenson LA, Pertwee RG, Henderson A, Toole J, Ellington HC (2002) Pharmacological characterization of the anandamide cyclooxygenase metabolite: prostaglandin E2 ethanolamide. *J Pharmacol Exp Ther* **301:** 900-907

Schlosburg JE, Carlson BL, Ramesh D, Abdullah RA, Long JZ, Cravatt BF, Lichtman AH (2009a) Inhibitors of endocannabinoid-metabolizing enzymes reduce precipitated withdrawal responses in THC-dependent mice. *AAPS J* **11:** 342-352

Schlosburg JE, Kinsey SG, Lichtman AH (2009b) Targeting fatty acid amide hydrolase (FAAH) to treat pain and inflammation. *AAPS J* **11:** 39-44

Varga K, Lake K, Martin BR, Kunos G (1995) Novel antagonist implicates the CB1 cannabinoid receptor in the hypotensive action of anandamide. *Eur J Pharmacol* **278:** 279-283

Weber A, Ni J, Ling KH, Acheampong A, Tang-Liu DD, Burk R, Cravatt BF, Woodward D (2004) Formation of prostamides from anandamide in FAAH knockout mice analyzed by HPLC with tandem mass spectrometry. *J Lipid Res* **45:** 757-763

Yang T (2003) Regulation of cyclooxygenase-2 in renal medulla. *Acta Physiol Scand* **177:** 417-421

Yu M, Ives D, Ramesha CS (1997) Synthesis of prostaglandin E2 ethanolamide from anandamide by cyclooxygenase-2. *J Biol Chem* **272:** 21181-21186

Zhu Q, Xia M, Wang Z, Li PL, Li N (2011) A novel lipid natriuretic factor in the renal medulla: sphingosine-1-phosphate. *Am J Physiol Renal Physiol* **301:** F35-41

Zou AP, Yang ZZ, Li PL, Cowley AJ (2001) Oxygen-dependent expression of hypoxia-inducible factor-1alpha in renal medullary cells of rats. *Physiol Genomics* **6:** 159-168

FOOTNOTES:

This work was supported by National Institutes of Health grants [DK54927] and [DA009789]; the Thomas and Kate Jeffress Memorial Foundation [J963]; VCU Clinical and Translational Science Award with support from the National Center for Research Resources and the A.D. Williams' Fund of the Virginia Commonwealth University [UL1RR031990].

This work was presented at the Federation of American Societies for Experimental Biology in San Diego, CA, April, 2012.

Address reprint requests to: Joseph K. Ritter, Ph.D., Associate Professor, 1217 E. Marshall St., KMSB Room 530, Department of Pharmacology and Toxicology, Virginia Commonwealth University, Box 980613, Richmond, VA 23298-0613. Email: jkritter@vcu.edu

FIGURE LEGENDS

Figure 1. Basal level of endocannabinoids and other fatty acid ethanolamine amides in the renal cortex and medulla. Lipids were extracted from samples of mouse renal cortex and medulla dissected from C57BL6 background mice and analyzed by LC-MS/MS. A. Levels of AEA and 2-arachidonoylglycerol (2-AG). Note the different scales for AEA and 2-arachidonoyl glycerol. B. Levels of palmitoyl ethanolamine (PEA) and oleoyl ethanolamine (OEA). The data represent the mean±SEM of n=6 mice per group. * Significant difference ($p<0.05$) compared to the cortex sample.

Figure 2. Expression of FAAH and COX-2 in the kidney. A. Western blot analysis of FAAH and COX-2 in microsomes prepared from the renal cortex and medulla of C57BL6 mouse kidneys. β-Actin antibody was used as a normalizing probe to control for differences in protein loading. B. Summarized data for the Western blot analysis of FAAH and COX-2 protein in microsomes prepared from the renal cortex or medulla of mouse kidneys presented as the mean ±SEM of the target band intensity normalized to β-actin. n=4 per group. * indicates a significant difference compared to the corresponding cortex sample ($p<0.05$). C. Immunohistochemical localization of FAAH and COX-2 in the renal cortex and medulla of control mice. Shown are representative images from analyses of kidneys from 3 mice at the indicated levels of magnification.

Figure 3. FAAH and COX-2 activity in the renal cortex and medulla. Microsomes from the renal cortex or medulla of C57BL6 mice were incubated with or without 100 μM AEA

(microsome rxn or microsomes only, respectively) for 30 minutes at 37°C. The reaction products were extracted and analyzed by LC-MS/MS as described under Methods. A. The rate of arachidonic acid formation, a measure of FAAH activity, determined by subtraction of the arachidonic acid values from reactions with and without AEA. n=6 per group. B. The rate of prostamide E2 formation in the same reactions. To the right of each panel are representative chromatograms for arachidonic acid or prostamide E2/D2 in reactions with and without AEA and microsomes from the renal cortex or medulla. * indicates a significant difference compared to the cortex sample ($p<0.05$). n=6 per group.

Fig. 4. Effect of intramedullary interstitial infusion of AEA on mean arterial pressure and renal water and sodium and potassium excretion in the absence or presence of a selective COX-2 inhibitor. U·V, urinary volume; UNa·V, urinary sodium excretion; UK·V, urinary potassium excretion; C, control infusion period; T, treatments with increasing AEA infusion rate (15, 30 or 60 nmol/kg/min). P, control infusion of post-treatment. One group of animals was infused intravenously with celecoxib (0.1 umol/min/kg) beginning with the control infusion period. * indicates a significant difference vs, respective control group ($P < 0.05$). n=6 per group.

Figure 5. Plasma clearance of AEA and prostamide E2. Intravenous bolus doses of AEA or prostamide E2 were administrated into mice, and plasma samples (50 µL) were then collected in EDTA tubes at timed post-dose intervals and analyzed for the indicated lipids by LC-MS/MS.

A. Plasma AEA concentrations after an AEA bolus (3.6 µmol/kg body weight). B. Plasma prostamide E2 levels after a prostamide E2 bolus (3.6 µmol/kg body weight). Values represent the mean±SEM of the lipid concentration in units of ng/mL. C. Representative chromatograms for prostamide E2 monitored using the 396/378 MRM showing prostamide E2 (in black)with accompanying formation of an unidentified isomeric metabolite which elutes slightly later (6.14 min) than prostamide E2 (5.51 min). n=4 per group.

Figure 6. Effect of prostamide E2 infusion on mean arterial pressure and renal blood flow. A. Representative tracings from a mouse given prostamide E2 by continuous intravenous infusion. Effects on MAP (black tracing) and RBF (gray tracing) are shown. The prostamide E2 infusion rate was 30, 60 or 120 nmol/kg/min. B. Summarized data for the average effect of prostamide E2 for each of the two 10 minute treatment periods at each infusion rate. * indicates a significant difference vs, control group ($P < 0.05$), n=7.

Figure 7. Angiotensin II i.v. dose response of mean arterial pressure and renal blood flow with and without prostamide E2 pretreatment in mice. A. Representative tracings showing the effect of an intravenous bolus injection of Ang II (50 ng/kg) and Ang II given after prostamide E2 pretreatment (120 nmol/kg/min) on MAP (black line) and RBF (gray line). B. Summarized data for acute bolus i.v. injection of Ang II in the absence and presence of prostamide E2 on MAP and RBF. The data are presented as the mean±SEM expressed as the % change from the basal level. C. Representative tracings showing the dose response of a continuous intravenous infusion of Ang II (5-20 ng/kg/min) and the effect of prostamide E2. D.

Summarized data for the effect of continuous intravenous infusion of Ang II with or without prostamide E2. * $p < 0.05$, **$p<0.01$, *vs.* control group. n=7.

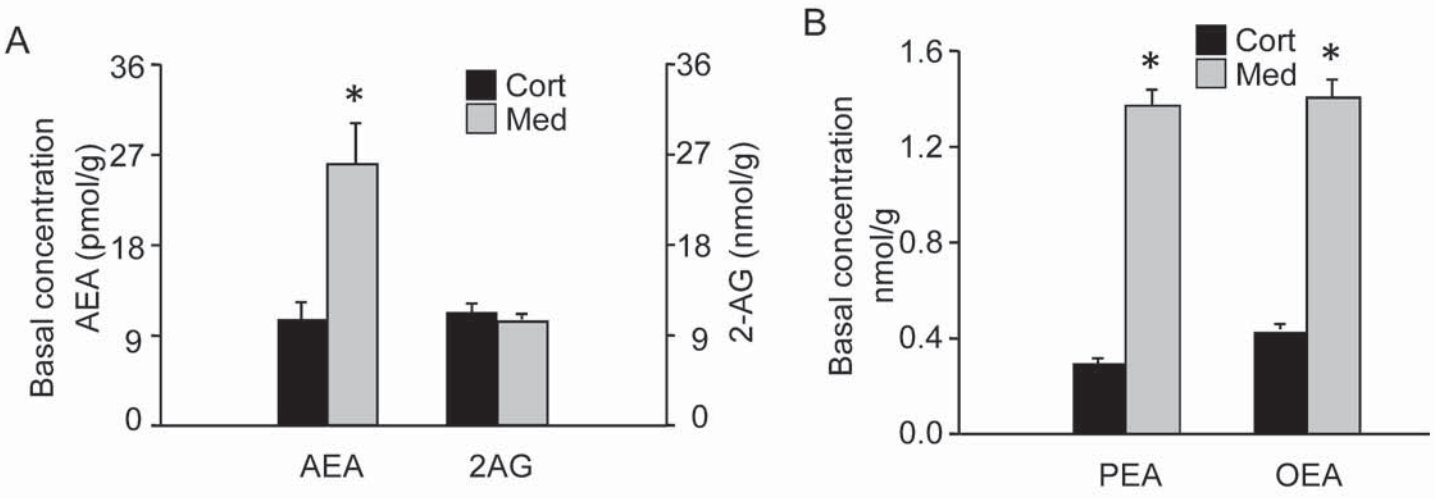
A
Basal concentration
AEA (pmol/g)
2-AG (nmol/g)
36
27
18
9
0
Cort
Med
*
AEA
2AG
B
Basal concentration
nmol/g
1.6
1.2
0.8
0.4
0.0
PEA
OEA

Fig. 1

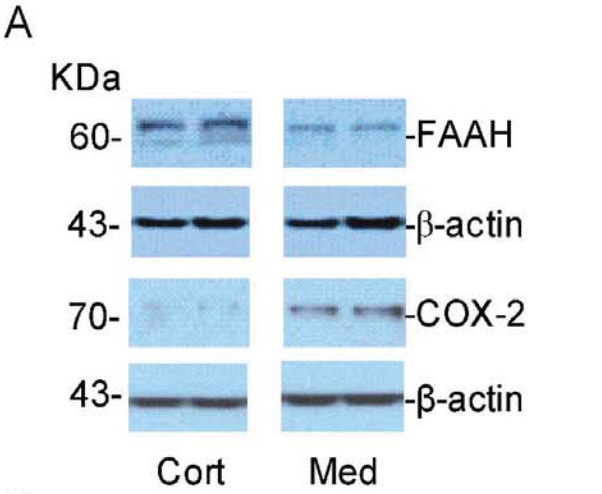
A
KDa
60-
-FAAH
43-
-β-actin
70-
-COX-2
43-
-β-actin
Cort
Med

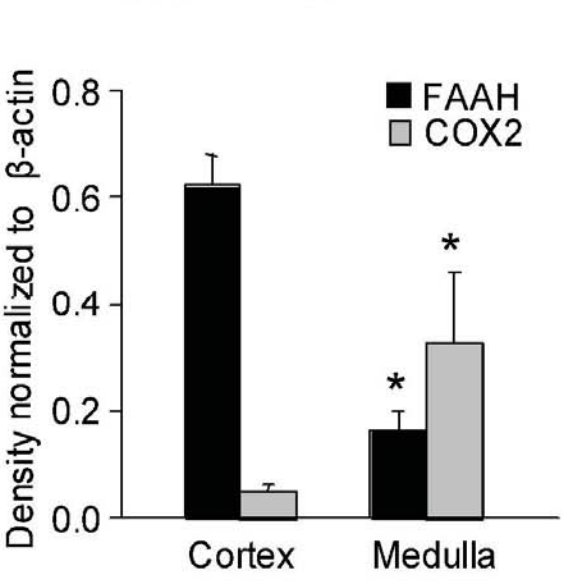
B
Density normalized to β-actin
0.8
0.6
0.4
0.2
0.0
FAAH
COX2
*
*
Cortex
Medulla

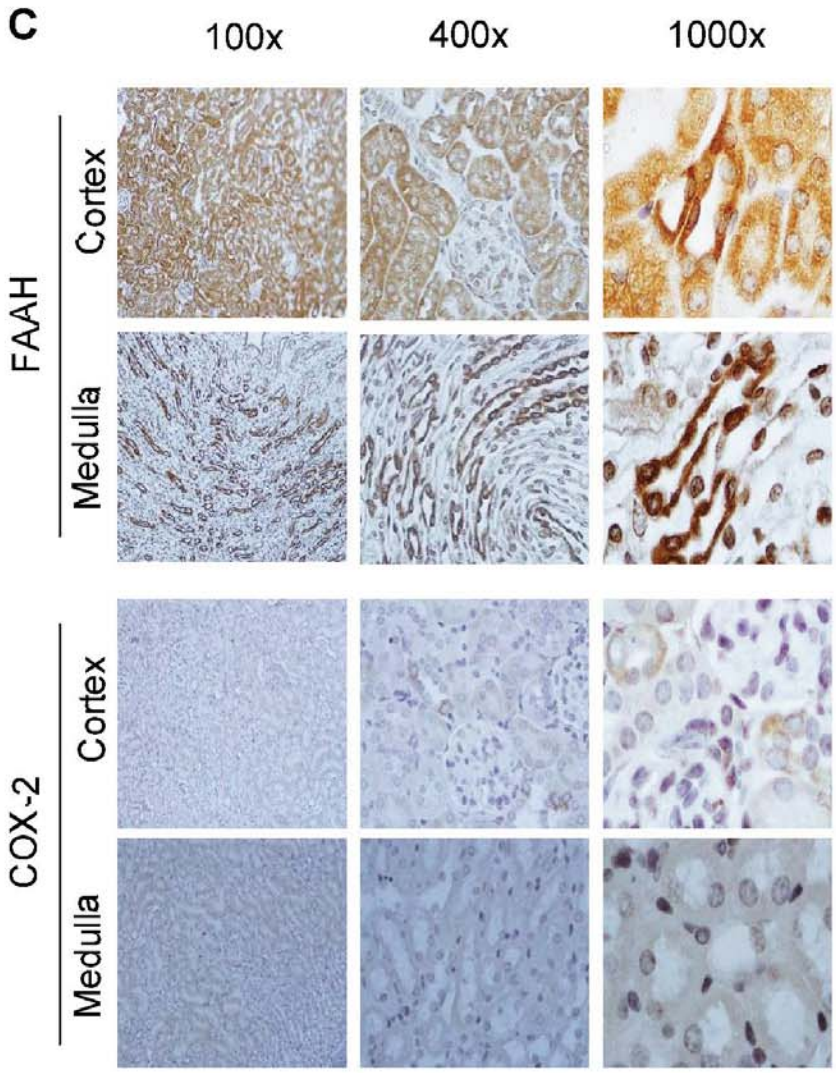
C
100x
400x
1000x
FAAH
Cortex
Medulla
COX-2
Cortex
Medulla

Fig. 2

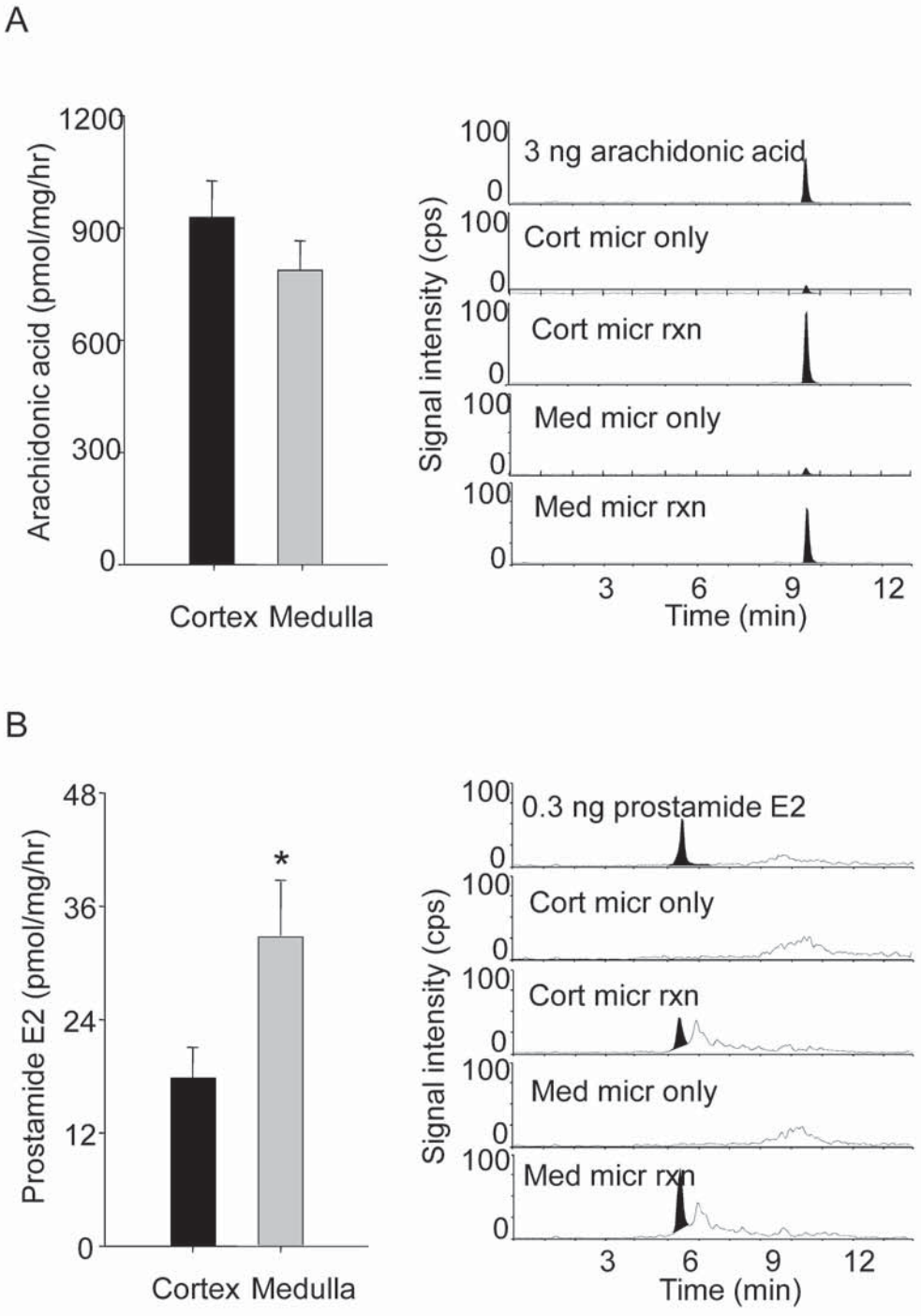
A
1200
900
600
300
0
Arachidonic acid (pmol/mg/hr)
Cortex Medulla
100
0
3 ng arachidonic acid
Cort micr only
Cort micr rxn
Med micr only
Med micr rxn
Signal intensity (cps)
3
6
9
12
Time (min)
B
48
36
24
12
0
*
Prostamide E2 (pmol/mg/hr)
Cortex Medulla
0.3 ng prostamide E2
Cort micr only
Cort micr rxn
Med micr only
Med micr rxn
Signal intensity (cps)
Time (min)

Fig. 3

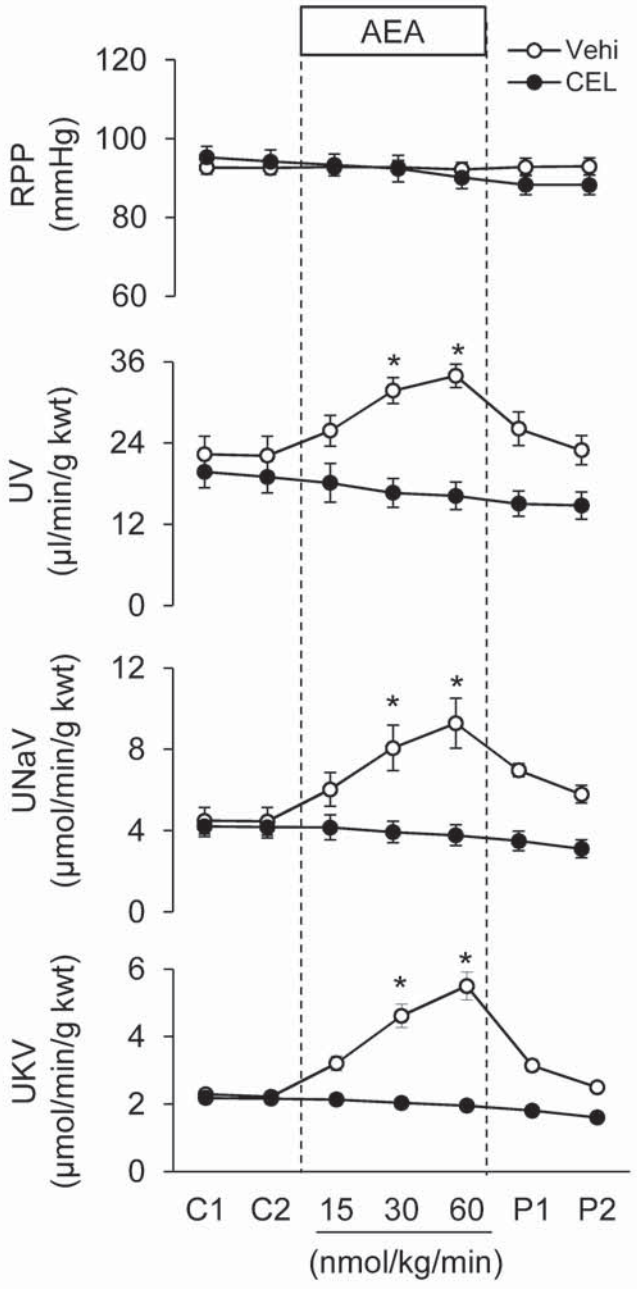
AEA
Vehi
CEL
RPP (mmHg)
120
100
80
60
UV (µl/min/g kwt)
36
24
12
0
UNaV (µmol/min/g kwt)
12
8
4
0
UKV (µmol/min/g kwt)
6
4
2
0
*
C1
C2
15
30
60
P1
P2
(nmol/kg/min)

Fig. 4

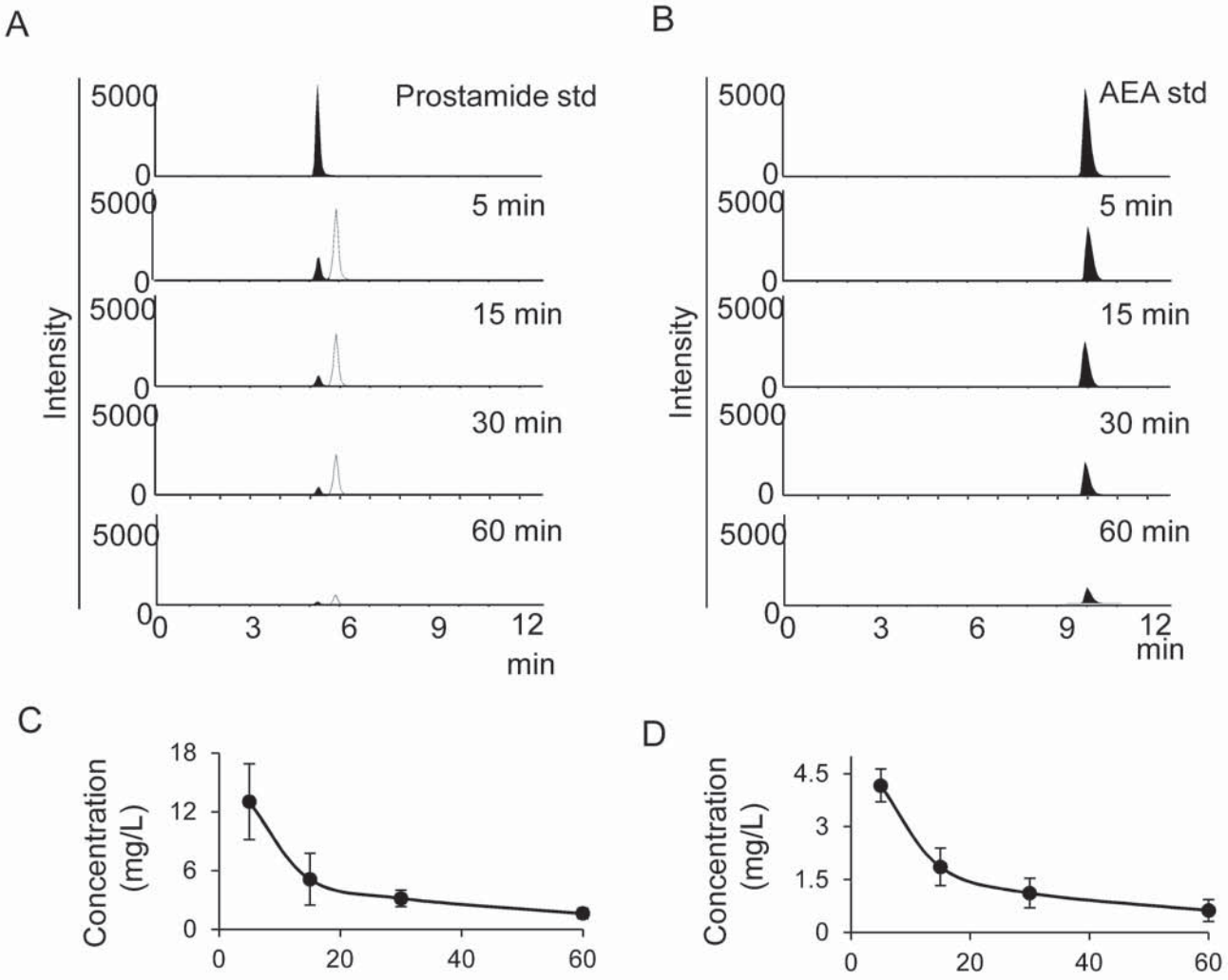
A
B
Prostamide std
AEA std
5 min
15 min
30 min
60 min
5000
0
Intensity
0
3
6
9
12
min
C
D
Concentration (mg/L)
18
12
6
0
4.5
3
1.5
0
20
40
60

Fig. 5

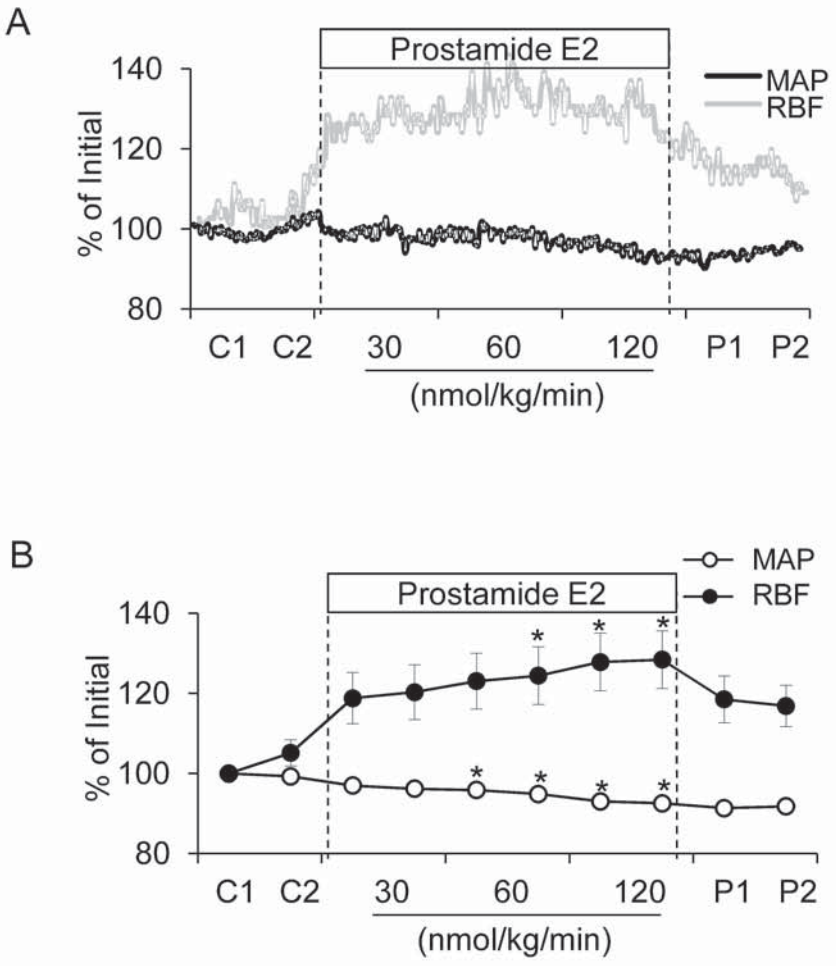
A
Prostamide E2
MAP
RBF
140
120
100
80
% of Initial
C1
C2
30
60
120
P1
P2
(nmol/kg/min)
B
Prostamide E2
MAP
RBF
140
120
100
80
% of Initial
C1
C2
30
60
120
P1
P2
(nmol/kg/min)

Fig. 6

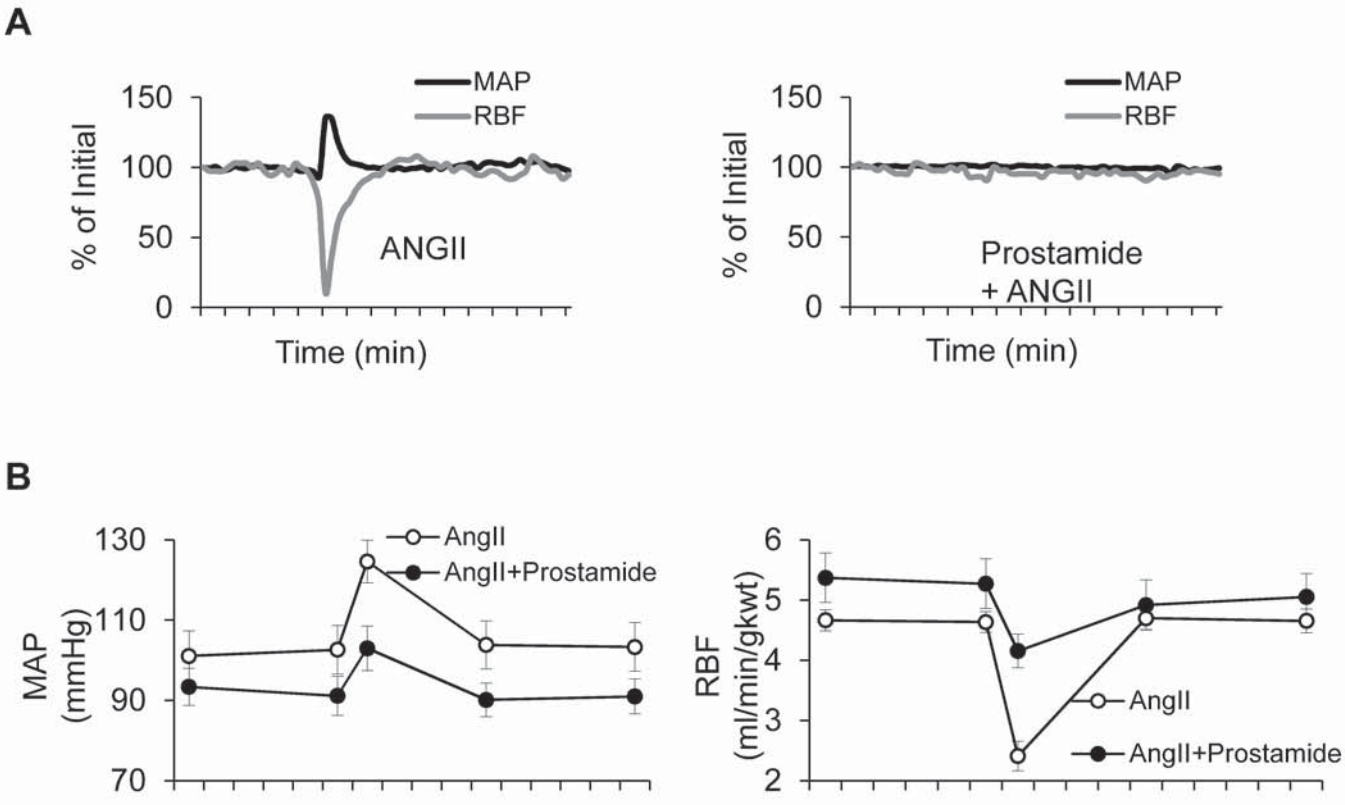
A
MAP
RBF
150
100
50
0
% of Initial
ANGII
Time (min)
MAP
RBF
150
100
50
0
% of Initial
Prostamide
+ ANGII
Time (min)
B
AngII
AngII+Prostamide
130
110
90
70
MAP
(mmHg)
6
5
4
3
2
RBF
(ml/min/gkwt)
AngII
AngII+Prostamide

Fig. 7A-7B

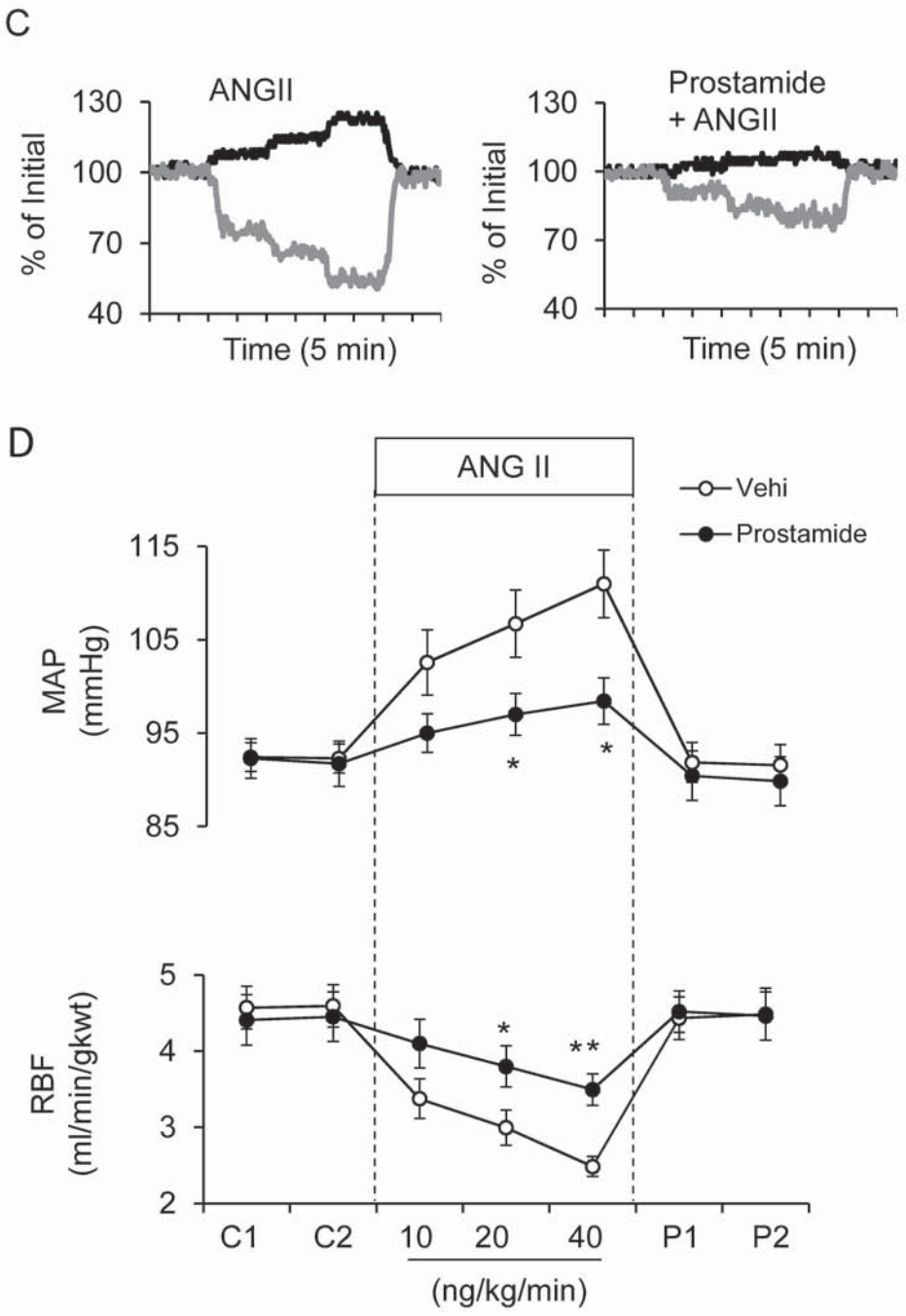
C
ANGII
Prostamide
+ ANGII
% of Initial
130
100
70
40
Time (5 min)
D
ANG II
Vehi
Prostamide
MAP
(mmHg)
115
105
95
85
RBF
(ml/min/gkwt)
5
4
3
2
*
**
C1
C2
10
20
40
P1
P2
(ng/kg/min)

Fig. 7C-7D